

Novel disordering mechanism in ferromagnetic systems with competing interactions

Juan Carlos Andresen,¹ Creighton K. Thomas,^{2,*} Helmut G. Katzgraber,^{2,1} and Moshe Schechter³

¹*Theoretische Physik, ETH Zurich, CH-8093 Zurich, Switzerland*

²*Department of Physics and Astronomy, Texas A&M University, College Station, Texas 77843-4242, USA*

³*Department of Physics, Ben Gurion University - Beer Sheva 84105, Israel*

(Dated: May 9, 2012)

We study the interplay between ferromagnetic and spin-glass phases in magnetic systems such as $\text{LiHo}_x\text{Y}_{1-x}\text{F}_4$ theoretically, as well as using numerical simulations of a three-dimensional diluted long-range dipolar Ising model with competing interactions in the presence of a random field. Our results suggest the existence of a novel disordering mechanism of the ferromagnetic phase due to the underlying spin-glass phase when a random field is applied. We numerically compute the zero-temperature phase boundary between the quasi-spin-glass and ferromagnetic phases as a function of the Ho concentration and random-field strength, and explain the peculiar linear dependence of the critical temperature on the strength of the random field found in recent experiments by Silevitch *et al.* [Nature **448**, 567 (2007)] on the $\text{LiHo}_x\text{Y}_{1-x}\text{F}_4$ compound.

PACS numbers: 75.50.Lk, 75.40.Mg, 05.50.+q, 64.60.-i

Introduction.— The random-field Ising model (RFIM) plays a central role in the study of disordered systems and has been applied to problems across disciplines ranging from disordered magnets to random pinning of polymers in two space dimensions, as well as water seepage in porous media.

At and below the lower critical dimension $d_\ell = 2$, the ferromagnetic (FM) phase is unstable to an infinitesimal random field [1, 2]. At higher space dimensions the disordering of the ferromagnetic phase requires the random field strength to be of the order of the strength of the interaction between the spins. Yet, the effect of the random field on the phase transition between the FM and paramagnetic (PM) phases—for systems with both short range and dipolar interactions—has been source of vast experimental and theoretical scrutiny over the last two decades; see Refs. [3–5] and references therein. Over the last three decades the RFIM has been studied experimentally via dilute antiferromagnets in a field [6], as both the random-field Ising model and the diluted antiferromagnetic Ising model in a field share the same universality class near criticality. More recently it has been shown that in anisotropic dipolar magnets the RFIM can be realized in the FM phase: By applying a transverse field to a dilute dipolar ferromagnet, such as $\text{LiHo}_x\text{Y}_{1-x}\text{F}_4$, one transforms the spatial disorder to an *effective* random field in the longitudinal direction [7–9]. This new possibility to study the RFIM in the FM phase opened the doors for advancing our understanding of the random field problem [10], as well as potential new applications, such as the advent of tunable domain-wall pinning [11] in magnetic materials.

Indeed, Silevitch *et al.* recently studied the FM-to-PM phase transition in the presence of random fields in the $\text{LiHo}_x\text{Y}_{1-x}\text{F}_4$ compound [12]. In particular, they found a peculiar behavior of the susceptibility as a function of the applied transverse field: A singularity in the field dependence of the critical temperature at zero field, as well as a *linear* dependence of the transition temperature on the effective random field strength (which is linear in the applied field for small fields [7, 9]). Similarly, in the molecular nanomagnet

$\text{Mn}_{12}-ac$ a strong suppression of the transition temperature as a function of the magnetic field was found [13]. However, in $\text{Mn}_{12}-ac$ it is unclear if for small fields the behavior is linear as well and singular as a function of the transverse field.

Both the $\text{LiHo}_x\text{Y}_{1-x}\text{F}_4$ and $\text{Mn}_{12}-ac$ systems, with small applied transverse magnetic fields, are well modeled by the RFIM. However, an important difference between the two systems is that the random field in the former is a result of spatial dilution, dictating a broad distribution of the interaction terms in both magnitude and sign, whereas in the latter the random field is a consequence of small random tilts in the spin direction. Therefore, it is unclear which “physical ingredients” are required such that the transition temperature depends linearly on the random field strength, and, in particular, which underlying mechanism dictates this behavior.

Here we study the interplay between FM and spin-glass (SG) phases in a dipolar Ising model with competing interactions in the presence of a random field. We find a novel disordering mechanism of the FM phase when a random field is applied and the system is in close proximity (e.g., via dilution) to an underlying SG phase. This disordering mechanism lies somewhat between the Imry-Ma and standard disordering mechanisms: The disordering of the FM phase occurs at a finite field, which is considerably smaller than the typical spin-spin interaction strength. At zero temperature we predict the existence of a FM-to-quasi-SG phase transition and numerically determine for $\text{LiHo}_x\text{Y}_{1-x}\text{F}_4$ the phase boundary as a function of the Ho concentration x and random field strength h . At finite temperature our theory is compatible with experiments at various Ho concentrations [12], suggesting that it is indeed the existence of competing interactions and the proximity to the SG phase that dictate the peculiar dependence of the critical temperature T_c on the random field strength h .

Theoretical analysis.— We first study the dilute $\text{LiHo}_x\text{Y}_{1-x}\text{F}_4$ system at zero temperature. For dilutions $x > x_c$ the system is FM, whereas for $x_0 < x < x_c$ the system is a spin glass (SG). Below we show numerically that $x_c \approx 0.3$. To date, it is unclear if $x_0 > 0$ [14, 15]. For $x \approx x_c$

we define the energy per spin of the lowest ferromagnetic state of the system as $f_{\text{FM}}(x)$; the lowest energy of the spin-glass state as $f_{\text{SG}}(x)$. Note that $f_{\text{FM}}(x)$ is the ground-state energy of the FM phase when $x > x_c$ and $f_{\text{SG}}(x)$ represents the ground-state energy of the SG phase for $x_0 < x < x_c$. At $x = x_c$ $f_{\text{FM}}(x_c) = f_{\text{SG}}(x_c)$, and for $x \approx x_c$, to first order in $x - x_c$, $f_{\text{SG}}(x) - f_{\text{FM}}(x) = \alpha(x - x_c) + \dots$. Consider the FM phase for $x > x_c$ and apply a random field of average strength h . For small random-field strength, the FM state in three dimensions cannot gain energy from the field, because domain flips are not energetically favorable. However, for spin glasses the lower critical (Imry-Ma) dimension is infinity [16] (no order in a field). In particular, in three space dimensions the energy of the system can be lowered by flipping domains, creating a quasi-spin-glass (QSG) phase with a finite correlation length. Thus, for x close enough to x_c the energy of the SG state will be lower than the energy of the FM state at a finite random field, which is still considerably smaller than the typical interaction strength between the spins. More generally, any three-dimensional Ising system with competing interactions having at zero random field a FM ground state and a SG state in a somewhat higher energy, will have a phase transition to the QSG phase as a function of the random field strength. The disordering of the ferromagnetic phase therefore occurs at a finite field whose magnitude depends on the proximity to the SG phase and, in particular, can be much smaller than the characteristic spin-spin interaction strength. Because in systems like $\text{LiHo}_x\text{Y}_{1-x}\text{F}_4$ the effective random fields are a result of quantum fluctuations [7, 17], this phase transition is a particular case of a quantum phase transition where the quantum fluctuations of the individual spins are small involving only the spin's ground and first excited states [18], but where the *collective effect* of all spins is strong enough to drive the transition.

The value of the critical random field can be estimated using the following Hamiltonian that describes a short-range Edwards-Anderson Ising spin glass [19] in a random field:

$$H_{\text{EA}} = - \sum_{\langle ij \rangle} J_{ij} S_i S_j + \sum_i h_i S_i. \quad (1)$$

In Eq. (1) J_{ij} are nearest-neighbor Gaussian random bonds between the spins S_i with zero mean and standard deviation J , and h_i are Gaussian random fields of average strength h [20]. The SG ground state is unstable to an infinitesimal random field, creating domains of typical size $(J/h)^{1/(3/2-\theta)}$, with $\theta \approx 0.2$ the stiffness exponent in three dimensions [21]. The energy reduction per spin resulting from the random field is thus of order $f(h) = h(J/h)^{-(3/2)/(3/2-\theta)}$. One can show that the total energy reduction per spin is of the same order, because the energy cost to flip domains is much smaller. The critical field $h_c(x)$ can be computed from $f(h = h_c) = f_{\text{SG}} - f_{\text{FM}} = \alpha(x - x_c)$ to obtain

$$h_c(x) = \alpha'(J)(x - x_c)^{\frac{3/2-\theta}{3-\theta}}, \quad (2)$$

where $\alpha'(J) = \alpha^{\frac{3/2-\theta}{3-\theta}} J^{\frac{3/2}{3-\theta}}$, see Fig. 1. For $h > h_c(x)$

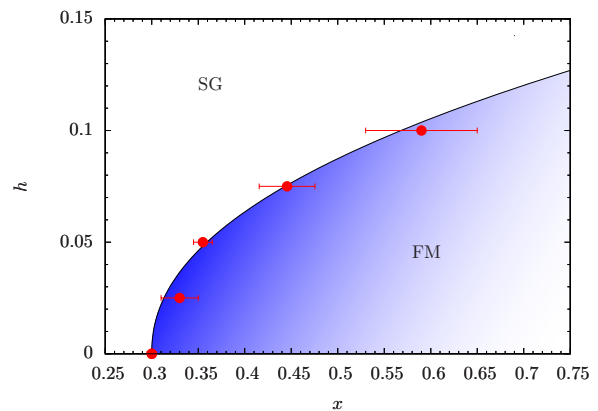


FIG. 1: (Color online) Comparison of the zero-temperature numerical and analytical [Eq. (2)] phase diagrams for the diluted dipolar Ising model [Eq. (4)] in the h - x plane. Using $\theta \approx 0.2$ [21] we obtain $h_c(x) \sim (x - x_c)^{0.464}$. The analytical prediction, Eq. (2), agrees very well with the numerical data with α' the only fitting parameter.

the system consists of finite-size domains within which short-range glassy order persists. The size of these domains decreases with increasing field, where at $h \approx J$ the system resembles a simple paramagnet. As $x \rightarrow x_c$ the disordering field approaches zero. For large $x - x_c$ and $h \approx J$ there is a crossover to the standard behavior where the disordering is a result of single-spin energy minimization, i.e., the intermediate QSG regime disappears.

When both T and $x - x_c$ are small but finite and the random field strength increases, the system changes first from the FM phase to the QSG phase, where the system is still dynamically frozen. Increasing the random field further, the QSG domain size decreases. The crossover to a disordered paramagnet is indicated by a peak in the magnetic susceptibility, which is broad and of finite magnitude, its width dictated by the typical domain size upon melting [7]. This scenario has been observed experimentally; see Fig. 2 of Ref. [12]. As the temperature is increased, the crossover to the PM regime occurs at smaller random fields, dictating larger typical domains and a higher peak for the magnetic susceptibility [7, 22].

Let us denote by T_{SG} the ordering temperature at zero random field of the underlying SG phase. For $T > T_{\text{SG}}$ the domain size at the crossover to the QSG phase is limited by $\xi_{\text{FM}} \propto (T - T_{\text{SG}})^{-\nu}$, where ν is the critical exponent of the correlation length. When the crossover field is small enough for ξ_{FM} to be reached, further increase in temperature leads to a smaller critical field h_c . However, the magnitude of the susceptibility peak saturates; see also Fig. 2 of Ref. [12].

To quantify the above observations and analyze the dependence of T_c on the effective random field, let us denote the lowest free energies of the FM phase below the critical FM temperature T_{FM} and a competing QSG phase, in which SG correlations exist within domains of size ξ , as $F_{\text{FM}}(x, T)$ and $F_{\text{QSG}}(x, T)$, respectively. Because the entropy of the QSG phase is dominated by the regions at the boundaries between domains [16], the main effect of the random fields is

to lower the energy of the QSG phase. Thus, $F_{\text{QSG}}(x, T) - F_{\text{FM}}(x, T) = -A(T - T_{\text{FM}}) + B(x - x_c) - h/\xi_{\text{QSG}}^{3/2}$. Here we used the fact that for $h = 0$ $F_{\text{QSG}}(x_c, T_c) = F_{\text{FM}}(x_c, T_c)$. We thus obtain

$$T_c(h) - T_c(0) = \frac{1}{A} \left[B(x - x_c) - h/\xi^{3/2} \right], \quad (3)$$

Equation (3) assumes that the FM phase is disordered by a QSG phase, in which domains of size ξ exist. Thus, it gives an upper bound for the value of $T_c(h)$. In fact, as we expect $T_c(h)$ to be a monotonous function, we expect the above expression for $T_c(h)$ to be valid at $h > h^*$, where $h^* = B(x - x_c)\xi^{3/2}$ is defined by the condition $T_c(h) = T_c(0)$. Our theoretical interpretation of the experimental data in Ref. [12] is in good agreement with our numerical results presented below for the $\text{LiHo}_x\text{Y}_{1-x}\text{F}_4$ system at different dilutions and magnetic fields. Both our theoretical and numerical results are consistent with $T_c(h)$ being linear in a regime where $h \ll J$, with deviation from linearity as $h \rightarrow 0$. Note that in Ref. [12] $T_c(h)$ is linear down to the lowest random fields studied if one defines the critical temperature by the asymptotic behavior of the susceptibility at high temperatures. However, if $T_c(h)$ is defined by the peak position of the susceptibility, deviations from linearity are observed at low fields [23].

Numerical details.— Previous work showed that $\text{LiHo}_x\text{Y}_{1-x}\text{F}_4$ at low temperatures and in the presence of an external transverse magnetic field is described by an effective Hamiltonian consisting of three terms [9, 24]: a long range term [dipolar, first term in Eq. (4)], an antiferromagnetic short range term [second term in Eq. (4)], and a longitudinal random field term [third term in Eq. (4)]. We thus study

$$\mathcal{H} = \sum_{i \neq j} \frac{J_{ij}}{2} \epsilon_i \epsilon_j S_i S_j + \frac{J_{\text{ex}}}{2} \sum_{\langle i, j \rangle} \epsilon_i \epsilon_j S_i S_j + \sum_i h_i \epsilon_i S_i. \quad (4)$$

Here $\epsilon_i = \{0, 1\}$ is the occupation of the magnetic Ho^{3+} ions on a tetragonal lattice (lattice constants $a = b = 5.175\text{\AA}$ and $c = 10.75\text{\AA}$) with four ions per unit cell [25, 26]. $S_i \in \{\pm 1\}$ are Ising spins, h_i represents the random fields drawn from a Gaussian distribution with zero mean and standard deviation h , where h is the strength of the applied field in [K]. The magnetostatic dipolar coupling J_{ij} between two Ho^{3+} ions is given by: $J_{ij} = D(r_{ij}^2 - 3z_{ij}^2)/r_{ij}^5$, where $r_{ij} = |\mathbf{r}_i - \mathbf{r}_j|$, \mathbf{r}_i is the position of the i -th Ho^{3+} ion and $z_{ij} = (\mathbf{r}_i - \mathbf{r}_j) \cdot \hat{z}$ is the component parallel to the easy-axis. The dipolar constant is $D/a^3 = 0.214\text{K}$ [27] and the antiferromagnetic nearest-neighbor exchange is set to $J_{\text{ex}} = 0.12\text{K}$ [25, 28]. We use periodic boundary conditions. The long-range interactions are taken into account via Ewald sums [26, 29]. At zero field and no dilution we find $T_c = 1.5316(2)\text{K}$, in excellent agreement with experimental results where $T_c = 1.530(5)\text{K}$ [30].

For the zero-temperature simulations [Fig. 1] we use (heuristic) jaded extremal optimization [31, 32]. For each run, we use exponents $\tau = 1.6, 1.8$ and 2 with an aging parameter $\Gamma = 0.05$ for at least 2^{26} steps. Empirically, ground states are found with high confidence for $L \leq 10$ and $h = 0$,

and $L \leq 8$ with small $h \neq 0$. Because the ground states of this model tend to be unique, we use the Binder ratio to identify the phase boundary. The Binder ratio is defined by $g = (1/2)(3 - [m^4]_{\text{av}} / [m^2]_{\text{av}}^2)$, where $m = (1/N) \sum_i S_i$ ($N = 4xL^3$ the number of spins) is the magnetization of the system and $[\dots]_{\text{av}}$ represents an average over the disorder. The Binder ratio is a dimensionless function and scales as $g \sim \tilde{G}[L^{1/\nu}(x - x_c)]$, allowing for the extraction of x_c and ν for a fixed value of h . Simulation parameters are listed in the supplementary material section, Table I.

At finite temperatures we use the parallel tempering Monte Carlo method [33]. Simulation parameters are listed in Tables II, III and IV in the supplementary material section. To determine the finite-temperature transitions for a given value of h and x we measure the two-point correlation length [34]

$$\xi_L = \frac{1}{2 \sin(k_{\text{min}}/2)} \sqrt{\frac{[\langle m^2(\mathbf{0}) \rangle_{\text{T}}]_{\text{av}}}{[\langle m^2(\mathbf{k}_{\text{min}}) \rangle_{\text{T}}]_{\text{av}}} - 1}, \quad (5)$$

where

$$m(\mathbf{k}) = \frac{1}{N} \sum_{i=1}^N S_i e^{i\mathbf{k} \cdot \mathbf{R}_i}. \quad (6)$$

Here $\langle \dots \rangle_{\text{T}}$ represents a thermal average, and \mathbf{R}_i is the spatial location of the spin S_i . $\mathbf{k}_{\text{min}} = (2\pi/L, 0, 0)$ represents the smallest nonzero wave vector. Near the transition ξ_L/L is dimensionless and expected to scale as $\xi_L/L \sim \tilde{X}[L^{1/\nu}(T - T_c)]$. Because at the transition temperature, $T = T_c$, the argument of the scaling function is zero (up to scaling corrections) and hence independent of L , we expect lines of different system sizes to cross at this point [Fig. 2(a)]. If however the lines do not meet, we know that no transition occurs in the studied temperature range [Fig. 2(c)]. To determine the critical temperature $T_c(h)$ we perform a finite-size scaling analysis of the data [see Fig. 2(b)]. Using a Levenberg-Marquardt minimization combined with a bootstrap analysis as described in Ref. [35] allows us to determine the optimal values of the critical parameters with a statistical error bar, see Table V.

Figure 1 shows the h - x phase diagram of the $\text{LiHo}_x\text{Y}_{1-x}\text{F}_4$ system at zero temperature. We find very good agreement with Eq. (2), using $\theta \approx 0.2$ [21], i.e. $h_c(x) \sim (x - x_c)^{0.464}$, and α' as a fitting parameter. Figure 3 shows finite-temperature data for different Ho-concentrations x . Panel 3(a) shows the critical temperature T_c as a function of the random field h for $x = 0.32$, i.e., $x - x_c = 0.02$ small. Our results at finite T corroborate our theoretical model where the FM phase disorders at $h \approx 0.045(5)$, a value slightly larger than found with the $T = 0$ simulations. We also find that $T_c(h)$ at low fields is well described by a linear behavior with possible deviations from linearity at very small fields, as suggested by our analytical considerations above. Both the disordering of the FM phase at small fields and the linearity of $T_c(h)$ seem to persist up to $x = 0.44$ [Fig. 3(b)], the dilution used in the experiments of Silevitch *et*

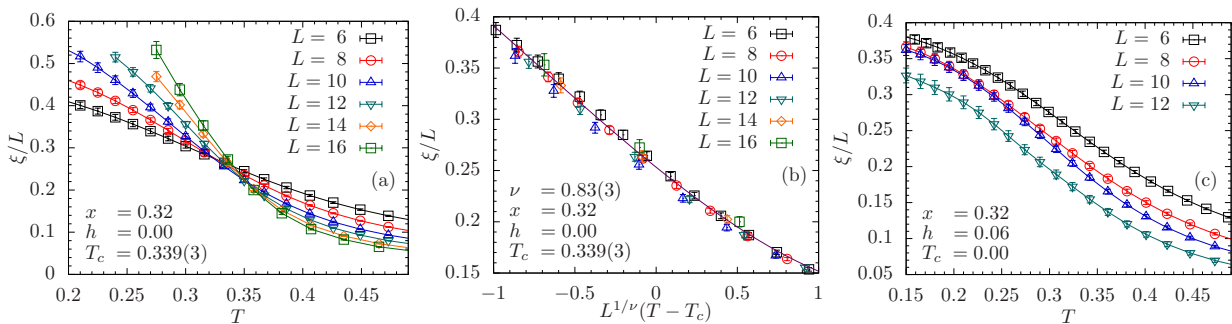


FIG. 2: (Color online) Finite-temperature data for the finite-size correlation length ξ_L/L as a function of temperature T and $x = 0.32$. (a) Data for $h = 0$. There is a clear crossing for $T_c = 0.340(3)$ [28] for different system sizes L . (b) Scaling analysis of the data for $h = 0$. The solid line corresponds to the optimal scaling function (polynomial approximation). (c) Data for $h = 0.06$. There is no sign of a transition.

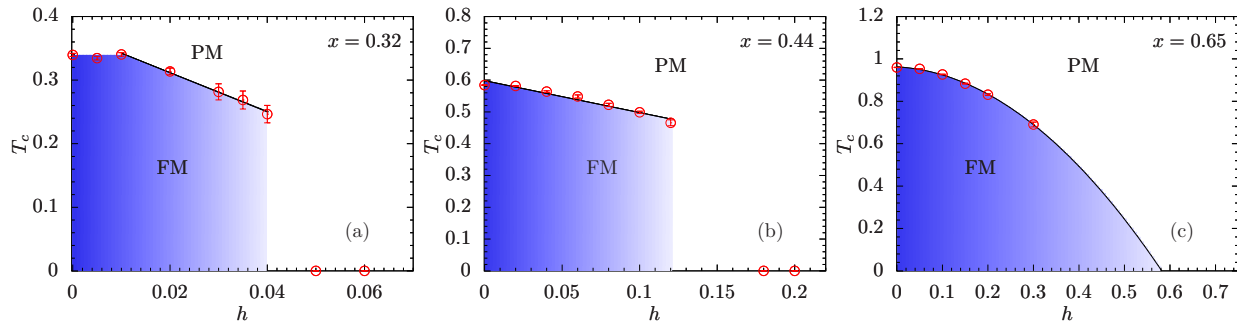


FIG. 3: (Color online) Critical temperature T_c [28] as a function of the random field strength h for different dilutions x . (a) $x = 0.32$. The critical temperature is linear in h . Moreover, above $h \approx 0.045(5)$ there is no sign of a phase transition. (b) Similar behavior as for $x = 0.32$ is found for $x = 0.44$ (dilution used in the experiments of Ref. [12]). (c) $x = 0.65$. At large dilutions $T_c(h)$ is quadratic in h .

al. [12]. For $x = 0.65$, i.e., far from the SG phase, [Fig. 3(c)] the behavior of $T_c(h)$ changes drastically to a clear quadratic dependence, suggesting a standard FM-PM transition at this concentration. Estimates of the critical parameters are listed in the supplementary material, Table V.

Note that our zero and finite-temperature analyses for zero random field suggest a temperature-independent critical concentration separating the FM and SG phases, i.e., the phase diagram for the $\text{LiHo}_x\text{Y}_{1-x}\text{F}_4$ system as a function of concentration and temperature does not contain a reentrant SG phase at zero field, in contrast to previous suggestions in the literature [36]. At the same time, our results at finite random fields at zero and finite temperatures for $x = 0.44$ and 0.65 suggest that there is a range of random fields where the system shows reentrance to a SG phase at low temperatures, a common effect found in glassy spin systems [37].

Conclusions.— We propose a novel disordering mechanism for three-dimensional ferromagnets with competing interactions and an underlying spin-glass phase. Furthermore, we explain various aspects of the experimental results of Silevitch *et al.* [12], including the peculiar linear dependence of the critical temperature on the applied transverse field. We further find that at smaller concentrations ($x = 0.32$, close to the spin-glass phase) the reduction of T_c with the random field becomes more pronounced. Our results strongly support the notion that it is the interplay between the competing inter-

actions and the induced effective random field that dictate the behavior of the $\text{LiHo}_x\text{Y}_{1-x}\text{F}_4$ ferromagnet at low concentrations. It would be interesting to study the generality of the above arguments with other anisotropic dipolar systems.

H.G.K. acknowledges support from the Swiss National Science Foundation (Grant No. PP002-114713) and the National Science Foundation (Grant No. DMR-1151387). M.S. acknowledges support from the Marie Curie Grant PIRG-GA-2009-256313. The authors thank ETH Zurich for CPU time on the Brutus cluster, and Amnon Aharony and Daniel Silevitch for useful discussions.

* Present address: Dept. of Materials Science and Engineering, Northwestern University, Evanston, Illinois 60208-3108, USA

- [1] Y. Imry and S.-K. Ma, Phys. Rev. Lett. **35**, 1399 (1975).
- [2] K. Binder, Z. Phys. B - Condensed Matter **50**, 343 (1983).
- [3] T. Nattermann, J. Phys. A **21**, L645 (1988).
- [4] D. P. Belanger, in *Spin Glasses and Random Fields*, edited by A. P. Young (World Scientific, Singapore, 1998), p. 251.
- [5] T. Nattermann, in *Spin Glasses and Random Fields*, edited by A. P. Young (World Scientific, Singapore, 1998), p. 277.
- [6] S. Fishman and A. Aharony, J. Phys. C **12**, L729 (1979).
- [7] M. Schechter and N. Laflorencie, Phys. Rev. Lett. **97**, 137204 (2006).
- [8] S. M. A. Tabei, M. J. P. Gingras, Y.-J. Kao, P. Stasiak, and J.-Y.

- Fortin, Phys. Rev. Lett. **97**, 237203 (2006).
- [9] M. Schechter, Phys. Rev. B **77**, 020401(R) (2008).
- [10] For a recent review and open problems see Ref. [38].
- [11] D. M. Silevitch, G. Aeppli, and T. F. Rosenbaum, PNAS **107**, 2797 (2010).
- [12] D. M. Silevitch, D. Bitko, J. Brooke, S. Ghosh, G. Aeppli, and T. F. Rosenbaum, Nature **448**, 567 (2007).
- [13] B. Wen, P. Subedi, L. Bo, Y. Yeshurun, M. P. Sarachik, A. D. Kent, A. J. Millis, C. Lampropoulos, and G. Christou, Phys. Rev. B **82**, 014406 (2010).
- [14] M. J. Stephen and A. Aharony, J. Phys. C **14**, 1665 (1981).
- [15] J. Snider and C. C. Yu, Phys. Rev. B **72**, 214203 (2005).
- [16] D. S. Fisher and D. A. Huse, Phys. Rev. B **38**, 386 (1988).
- [17] M. Schechter, P. C. E. Stamp, and N. Laflorencie, J. Phys. Cond. Mat. **19**, 145218 (2007).
- [18] The time-reversed state is not involved in this process [7].
- [19] K. Binder and A. P. Young, Rev. Mod. Phys. **58**, 801 (1986).
- [20] Our results remain unchanged if dipolar interactions in a random system are used, and when short-range exchange interactions are included as is the case for $\text{LiHo}_x\text{Y}_{1-x}\text{F}_4$.
- [21] A. K. Hartmann, Phys. Rev. E **59**, 84 (1999).
- [22] W. Wu, D. Bitko, T. F. Rosenbaum, and G. Aeppli, Phys. Rev. Lett. **71**, 1919 (1993).
- [23] D. M. Silevitch, private communication.
- [24] P. B. Chakraborty, P. Henelius, H. Kjnsberg, A. W. Sandvik, and S. M. Girvin, Phys. Rev. B **70**, 144411 (2004).
- [25] A. Biltmo and P. Henelius, Europhys. Lett. **87**, 27007 (2009).
- [26] K.-M. Tam and M. J. P. Gingras, Phys. Rev. Lett. **103**, 087202 (2009).
- [27] A. Biltmo and P. Henelius, Phys. Rev. B **76**, 054423 (2007).
- [28] All estimates of T_c and values of h are in Kelvin [K].
- [29] Z. Wang and C. Holm, J. Chem. Phys. **115**, 6351 (2001).
- [30] G. Mennenga, L. J. de Jongh, and W. J. Huiskamp, J. Magn. Magn. Mater. **44**, 59 (1984).
- [31] S. Boettcher and A. G. Percus, Phys. Rev. Lett. **86**, 5211 (2001).
- [32] A. A. Middleton, Phys. Rev. E **69**, 055701(R) (2004).
- [33] K. Hukushima and K. Nemoto, J. Phys. Soc. Jpn. **65**, 1604 (1996).
- [34] H. G. Ballesteros, A. Cruz, L. A. Fernandez, V. Martin-Mayor, J. Pech, J. J. Ruiz-Lorenzo, A. Tarancon, P. Tellez, C. L. Ullod, and C. Ungil, Phys. Rev. B **62**, 14237 (2000).
- [35] H. G. Katzgraber, M. Krner, and A. P. Young, Phys. Rev. B **73**, 224432 (2006).
- [36] D. H. Reich, B. Ellman, J. Yang, T. F. Rosenbaum, G. Aeppli, and D. P. Belanger, Phys. Rev. B **42**, 4631 (1990).
- [37] C. K. Thomas, D. A. Huse, and A. A. Middleton, Phys. Rev. Lett. **107**, 047203 (2011).
- [38] M. J. P. Gingras and P. Henelius, J. Phys.: Conf. Ser. **320**, 012001 (2011).

Supplementary Material: Andresen *et al.*

TABLE I: Simulation parameters for $T = 0$: System of size $L = 6, 8,$ and 10 , field h and dilution x are studied. x_{\min} [x_{\max}] is the smallest [largest] concentration studied and Δx is the step size between measurements. N_{sa} is the number of disorder realizations.

h	x_{\min}	x_{\max}	Δx	N_{sa}
0.000	0.280	0.350	0.010	5000
0.025	0.275	0.400	0.025	3000
0.050	0.300	0.400	0.025	3000
0.075	0.300	0.600	0.050	1500
0.100	0.400	0.800	0.100	1500

TABLE II: Simulation parameters at finite temperature and $x = 0.32$ for different fields h and system sizes L . The equilibration/measurement times are 2^b Monte Carlo sweeps. T_{\min} [T_{\max}] is the lowest [highest] temperature used and N_T is the number of temperatures. N_{sa} is the number of disorder realizations.

x	h	L	b	T_{\min}	T_{\max}	N_T	N_{sa}
0.32	0.000	6	15	0.100	0.500	25	2000
0.32	0.000	8	17	0.100	0.500	25	2000
0.32	0.000	10	18	0.168	0.500	20	1000
0.32	0.000	12	18	0.240	0.500	15	1000
0.32	0.000	14	16	0.275	0.500	10	750
0.32	0.000	16	16	0.275	0.500	10	385
0.32	0.005	6	12	0.280	0.550	20	2000
0.32	0.005	8	13	0.280	0.550	20	3500
0.32	0.005	10	15	0.280	0.550	20	2000
0.32	0.005	12	17	0.280	0.550	20	1200
0.32	0.005	14	16	0.312	0.550	17	1200
0.32	0.010	6	15	0.050	0.500	30	1500
0.32	0.010	8	17	0.050	0.500	30	1100
0.32	0.010	10	18	0.230	0.500	15	1000
0.32	0.010	12	19	0.245	0.500	15	850
0.32	0.010	14	17	0.265	0.500	15	750
0.32	0.020	6	15	0.050	0.500	30	1500
0.32	0.020	8	18	0.050	0.500	30	1000
0.32	0.020	10	16	0.245	0.500	15	1000
0.32	0.020	12	19	0.245	0.500	15	600
0.32	0.020	14	17	0.274	0.500	13	7500
0.32	0.030	6	14	0.226	0.450	14	3000
0.32	0.030	8	17	0.212	0.450	15	2000
0.32	0.030	10	17	0.226	0.450	14	2000
0.32	0.030	12	19	0.226	0.450	14	600
0.32	0.035	6	13	0.218	0.450	20	3000
0.32	0.035	8	14	0.218	0.450	20	2000
0.32	0.035	10	15	0.218	0.450	20	2000
0.32	0.035	12	18	0.218	0.450	20	650
0.32	0.040	6	14	0.218	0.450	20	3000
0.32	0.040	8	16	0.218	0.450	20	2800
0.32	0.040	10	17	0.218	0.450	20	2000
0.32	0.040	12	17	0.218	0.450	14	1000
0.32	0.050	6	13	0.100	0.650	35	4500
0.32	0.050	8	16	0.100	0.650	35	3000
0.32	0.050	10	18	0.100	0.650	35	1000
0.32	0.060	6	15	0.100	0.650	35	4000
0.32	0.060	8	16	0.150	0.500	20	1000
0.32	0.060	10	18	0.150	0.500	20	1000
0.32	0.060	12	17	0.150	0.500	20	1000

TABLE III: Simulation parameters at finite temperature and $x = 0.44$. For details see Table II.

x	h	L	b	T_{\min}	T_{\min}	N_T	N_{sa}
0.44	0.000	6	10	0.500	1.000	30	1000
0.44	0.000	8	12	0.500	1.000	30	1300
0.44	0.000	10	13	0.500	1.000	30	2500
0.44	0.000	12	14	0.500	1.000	30	550
0.44	0.000	14	14	0.560	1.000	47	650
0.44	0.020	6	10	0.525	0.800	30	2000
0.44	0.020	8	12	0.525	0.800	30	2000
0.44	0.020	10	13	0.525	0.800	30	1000
0.44	0.020	12	14	0.525	0.800	30	1000
0.44	0.020	14	14	0.550	0.800	30	900
0.44	0.040	6	11	0.525	0.750	22	2000
0.44	0.040	8	12	0.525	0.750	22	2000
0.44	0.040	10	14	0.540	0.750	20	1000
0.44	0.040	12	15	0.550	0.750	20	1000
0.44	0.060	6	11	0.500	0.750	25	2000
0.44	0.060	8	13	0.500	0.750	25	2000
0.44	0.060	10	13	0.519	0.730	19	2000
0.44	0.060	12	14	0.519	0.730	19	1300
0.44	0.080	6	12	0.475	0.725	20	2000
0.44	0.080	8	13	0.475	0.725	20	2000
0.44	0.080	10	13	0.500	0.725	20	1200
0.44	0.080	12	14	0.509	0.725	19	1300
0.44	0.100	6	13	0.445	0.725	23	2000
0.44	0.100	8	14	0.445	0.725	23	2300
0.44	0.100	10	13	0.445	0.725	23	2200
0.44	0.100	12	15	0.475	0.725	20	880
0.44	0.120	6	11	0.445	0.725	23	2500
0.44	0.120	8	12	0.445	0.725	23	2200
0.44	0.120	10	13	0.445	0.725	25	1000
0.44	0.120	12	14	0.445	0.725	25	1000

TABLE IV: Simulation parameters at finite temperature and $x = 0.65$. For details see Table II.

x	h	L	b	T_{\min}	T_{\min}	N_T	N_{sa}
0.65	0.000	6	10	0.500	1.400	20	1000
0.65	0.000	8	12	0.500	1.400	20	500
0.65	0.000	10	12	0.500	1.400	20	450
0.65	0.000	12	11	0.500	1.400	20	500
0.65	0.000	14	10	0.850	1.400	15	490
0.65	0.000	16	11	0.850	1.400	15	470
0.65	0.050	6	8	0.697	1.400	15	1000
0.65	0.050	8	10	0.697	1.400	15	500
0.65	0.050	10	9	0.800	1.400	20	500
0.65	0.050	12	11	0.697	1.400	15	300
0.65	0.050	14	10	0.900	1.400	15	500
0.65	0.050	16	11	0.920	1.400	16	280
0.65	0.010	6	8	0.820	1.400	20	750
0.65	0.010	8	9	0.820	1.400	20	500
0.65	0.010	10	10	0.820	1.400	20	500
0.65	0.010	12	11	0.820	1.400	20	800
0.65	0.010	14	12	0.820	1.400	20	380
0.65	0.015	6	8	0.820	1.400	20	1000
0.65	0.015	8	10	0.820	1.400	20	500
0.65	0.015	10	11	0.820	1.400	20	500
0.65	0.015	12	12	0.820	1.400	20	500
0.65	0.015	14	13	0.820	1.400	20	500
0.65	0.020	6	10	0.661	1.400	15	500
0.65	0.020	8	11	0.661	1.400	15	400
0.65	0.020	10	14	0.756	1.400	13	1300
0.65	0.020	12	15	0.756	1.400	13	1000
0.65	0.020	14	16	0.756	1.400	13	990
0.65	0.030	6	10	0.600	1.400	20	750
0.65	0.030	8	15	0.600	1.400	20	1000
0.65	0.030	10	17	0.600	1.400	20	550
0.65	0.030	12	19	0.600	1.400	20	530

TABLE V: Critical parameters estimated using a finite-size scaling technique: For each concentration x and field strength h we compute the critical temperature T_c and critical exponent ν .

x	h	T_c	ν
0.32	0.000	0.340(3)	0.83(3)
0.32	0.005	0.335(3)	0.89(3)
0.32	0.010	0.340(3)	0.81(3)
0.32	0.020	0.314(5)	1.04(7)
0.32	0.030	0.281(13)	1.23(17)
0.32	0.035	0.269(14)	1.31(19)
0.32	0.040	0.247(14)	1.41(15)
0.44	0.000	0.584(1)	0.75(1)
0.44	0.020	0.581(1)	0.70(1)
0.44	0.040	0.563(3)	0.77(2)
0.44	0.060	0.548(5)	0.86(3)
0.44	0.080	0.522(5)	0.99(4)
0.44	0.100	0.506(5)	1.01(4)
0.44	0.120	0.466(9)	1.39(12)
0.65	0.000	0.9597(8)	0.79(2)
0.65	0.050	0.9531(10)	0.76(2)
0.65	0.010	0.9264(14)	0.84(3)
0.65	0.015	0.8832(21)	0.91(4)
0.65	0.020	0.8312(41)	1.06(10)
0.65	0.030	0.6905(113)	1.11(12)